



International Journal of Engineering Research and Science & Technology

ISSN : 2319-5991
Vol. 4, No. 2
May 2015



www.ijerst.com

Email: editorijerst@gmail.com or editor@ijerst.com

Research Paper

NUMERICAL SIMULATION OF THERMOMECHANICAL BEHAVIOR OF EVAPORATORS FAN IN A NEGATIVE COLD ROOM

IBOM-IBOM Aloys-Marie¹, EDOUN Marcel^{1*}, KUITCHE Alexis¹

*Corresponding Author: **EDOUN Marcel** ✉ edounmarcel@yahoo.fr

This work is a contribution to the study of the influence of the operating cycle of a negative cold room on the thermomechanical behavior of evaporators fan blades. The objective was to demonstrate the effect of cyclic and continuous variation of the operating temperature of 20°C to -20°C on the appearance of cracks on the fan blades. Throughout this study, the effects of mechanical vibration have been neglected. The temperature gradient and the stress field in the material was estimated using Hoai model. Bueckner and Paris model was used to evaluate the stress intensity factor in order to determine the lifespan of the fan blades on the evaporator of the freezer rooms. The equation system chosen was solved by the application of the method of separated variables and dichotomy. The results show that the temperature field generated by either a short or long operating cycle does not have a considerable effect on the thermomechanical behavior of the fans. The breakage of the fans may occur after minutes and minutes respectively during operation of the freezer room's short cycle and long cycle.

Keywords: Thermomechanical, Model, Breakage, Negative cold room

INTRODUCTION

A negative cold chamber is a chamber equipped with a refrigeration machine (evaporation machine and absorption of a liquefiable gas) which keeps the temperature at the heart of the refrigerated goods at -18°C. This method of preservation by artificial cold is widely used in the agro-industry. It will greatly reduce the activity of the water during the storage period, as well as microbiological activity while minimising the physical and

chemical changes of foodstuffs (Khama *et al.*, 2009). These refrigerating machines consist of one or more compressor (s), condenser (s), valve (s) and evaporator (s). The evaporator is the most important part of this machine: it is at the evaporator that cold is produced by absorbing heat from the surrounding environment. For industrial applications, mid-sized and large capacity, evaporators are equipped with one or more fans to homogenize the temperature

¹ Laboratory of Energetic and Applied Thermal Process, Department of Energetic, Electrical and Automatic Engineering, National School of Agro-Industrial Sciences, University of Ngaoundere, PO Box 455 Ngaoundere-Cameroon.

distribution and accelerate the cooling of the stored products.

In tropical areas, we have noted frequent interruptions in the cold chain of food products due to the cracking and breaking of evaporator fan blades.

Indeed, when a metal is cyclically subject to local variations in temperature, compressions and expansions appear leading to mechanical loads. These loads when recurrent, may lead to cracking of the blades and finally to the breakdown of the metal (Vincent *et al.*, 2005).

In the literature, many studies focus on the description of the breakdown of certain materials. Saane (2008) worked on the study of plastic deformation of ferrite at temperatures below -68°C . Simulating the dynamics of dislocations (occurrence of cracks), he shows that individual dislocations in pressure vessel steel is dependent on temperature and strain rate. Laforte (2001) studied the deformation to adhesive rupture by traction, bending and torsion of a frosted substrate and shows that the break is always preceded by a boot (crack) and a ductile propagation. Obrtlík *et al.* (2005) defined two deformation regimes: one valid at higher temperatures, characterised as “a thermal” the second for very low temperatures (up to -196°C) and characterised as “athermal” For a strain rate of the order of 10^{-4}S^{-1} , the athermal temperature is close to room temperature. Work done on 16MND5 pressure vessel steels show that the damage is due to the presence of inclusion, germination of a second population and coalescence mechanisms (Tanguy and Besson, 2012). This work has been conducted either by increasing or by lowering the temperature constant of the material. However, cold rooms

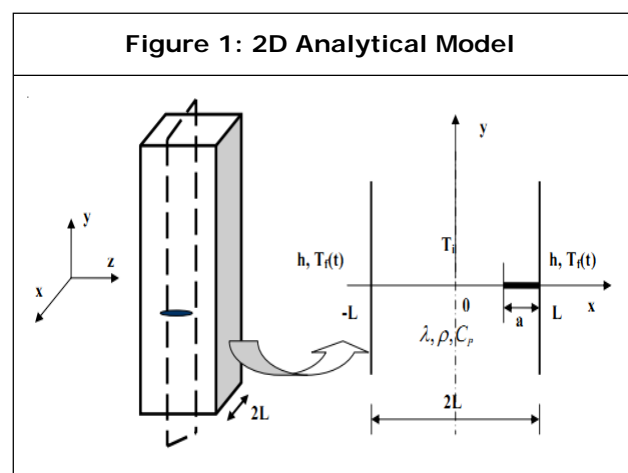
and freezer rooms especially have a thermal operating regime that is akin to a saw tooth: Cooling (during compressor operation) and defrost (when operating heating resistors). To the best of our knowledge, there are no studies on the effect of the cyclic variation of temperature on the thermo-mechanical behavior of metal, hence the importance of this work.

The objective of this study is to demonstrate using a numerical simulation, the effect of the cyclic variation of the operating temperature of a negative cold room on the appearance of cracks on the fan blades installed on the evaporators.

MATERIALS AND METHODS

Description of Problem

Figure 1 is a simplified representation of the analytical model of our sample in two dimensions. The sample is a metal of length $2L$, having an initial temperature and whose two ends are homogeneously cooled at a constant temperature with a heat transfer coefficient h : this is a problem of heat transfer by forced convection between the fluid and a plate. The two-dimensional study is carried out along the xy plane of symmetry.



The equation (1) describes this heat transfer problem:

$$\left\{ \begin{array}{l} \left(\frac{\partial T}{\partial t}\right) - \frac{k}{\rho c_p} \left(\frac{\partial^2 T}{\partial x^2}\right) = 0 \\ T(x, t=0) = T_0, t > 0 \\ -k \left(\frac{\partial T(x = \pm L, t)}{\partial x}\right) = \pm h(T(x = \pm L, t) - T_{ext}) \end{array} \right. t > 0 \quad \dots(1)$$

To determine the time it takes for cracks to appear on our sample, we need to evaluate the temperature field in the sample and deduce the associated strain field. Then, calculate the stress intensity factor which plays an important role in the thermal fatigue of metals (Bueckner, 1970) and finally, determine the number of cycles using the propagation law.

Evaluation of the Temperature Field

According to Hoai (2009), the temperature field which characterizes the evolution of the temperature in the thickness of a metal at a time *t* is given by the equations (2) and (3).

$$\frac{T(x, t) - T_f}{T_i - T_f} = \sum_{n=0}^{\infty} \left[\left(\frac{2 \sin(k_n)}{k_n + \sin(k_n) \cos(k_n)} \right) \cos\left(k_n \frac{x}{L}\right) e^{-k_n^2 \frac{Dt}{L^2}} \right] \quad \dots(2)$$

with $k_n \text{tg}(k_n) = Bi \quad \dots(3)$

Evaluation the Elastic Strain Field

In order to evaluate the elastic strain field induced by a temperature field, we used the linear thermoelastic behavior law. This law determines the parameter responsible for the appearance of cracks in the metal according to expression (4).

$$\frac{\sigma_{yy}(x, t)}{E\alpha} = \frac{1}{(1-\nu)} \left[\frac{\int_0^L T(x, t) dx}{L} T(x, t) \right] \quad \dots(4)$$

Estimation of Blades Breaking Times

Determining the time it takes before the blades break depends on the strain intensity factor and the number of complete cycles of operation of the negative cold room in the time interval considered. It is the force exerted on the material before failure (Rice, 1972). It derives from the stress field and is of the form of equation (5).

$$K_I(t) = \frac{2L}{\sqrt{\pi a}} \int_{1-\frac{a}{L}}^1 \frac{F_I\left(\frac{x}{L}, \frac{a}{L}\right), \sigma_{yy}\left(\frac{x}{L}, t\right)}{\left(1 - \frac{a}{2L}\right)^{1.5} \sqrt{1 - \left(\frac{(L-x)^2}{a^2}\right)}} d\left(\frac{x}{L}\right) \quad \dots(5)$$

The function $F_I\left(\frac{x}{L}, \frac{a}{L}\right)$ is defined by the Tada model (1985)

The law of propagation as defined by Tavassoli (1995) is chosen to determine the number of complete operation cycles (N) of the cold room in the time interval considered. It is given by the relation (6).

$$\frac{da}{dN} = C \Delta K^m \quad \dots(6)$$

The product of the number of complete operation cycles of the cold room until time t and of the period of a cycle (T) was used to estimate the sample breaking time. This time is given as follows:

$$D.V.P. = N \times T \quad \dots(7)$$

Numerical Method

Solving the equations that describe the evolution of the temperature field of elastic strain in the thickness of a material (evaporator fan blades) requires numerical methods. In this study, we applied the finite element method to solve the equations (2) to (5).

RESULTS AND DISCUSSION

Characterization of the Temperature Profile in the Cold Room

The characterization of the negative cold room temperature profile helped identify three operating cycles of the cold room: a short cycle, a long cycle and a cycle of maintenance shutdown. In truth we were just interested in the first two cycles.

Case of a Short Operating Cycle

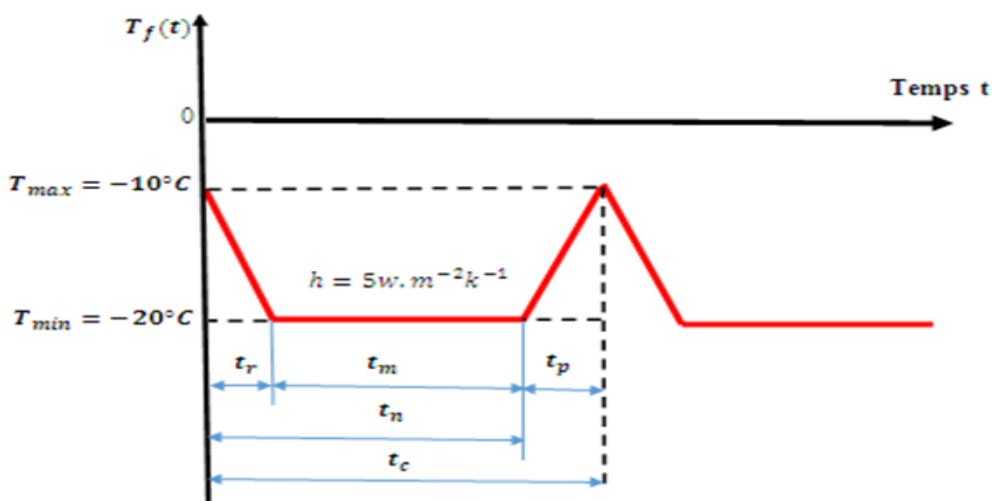
A short cycle is the daily variation cycle of the operating temperature of the negative cold room with defrost heaters. Figure 2 shows that function $T_f(t)$ consists of three temperature stages: cooling, constant rate and the defrosting.

Cooling: The sample is cooled by a stream of air having a coefficient of heat exchange $h=5w.m^{-2}k^{-1}$ and the temperature drops linearly from $T_{max} = -10^{\circ}C$ to $T_{min} = -20^{\circ}C$ during the cooling period $t_r = 22$ min.

Constant Temperature: During the period $t_m = 260$ min the air stream temperature is considered a constant.

Defrost: The sample is crossed by a stream of hot air which keeps the same coefficient of thermal exchange $h=5w.m^{-2}k^{-1}$, but this time with the temperature which linearly increases from $T_{min} = -20^{\circ}C$ to $T_{max} = -10^{\circ}C$ during the defrost period $t_p = 22$. This was then allowed to set the length of a short cycle $t_c = t_r+t_m+t_p$.

Figure 2: Temperature profile evolution in case of a short operating cycle



The analytical expression of the Tf(t) is given by the expression (8)

$$T_f(t) = \left(-\frac{10}{22}t - 10\right)[u(t) - u(t - 22)] + (-20)[uu(t - 22) - u(t - 262)] + \left(\frac{10}{22}t - \frac{3050}{22}\right)u(t - 262) - u(t - 284) \dots(8)$$

Case of a Long Operating Cycle

Figure 3 shows that the Tf(t) consists of seven segments: a quench, an operation at a constant rate (-20°C), a sudden warming up to -10°C, an operation at a constant rate at -10°C, a new cooling down to -20°C, again constant operation

at -20°C and finally a sudden warming up to a temperature of 20°C. The expression of this function is given by equation (9).

$$T_f(t) = (-20)[u(t) - u(t - 129600)] + (-10)[u(t - 129600) - u(t - 172800)] + (-20)[u(t - 172800) - u(t - 302400)] \dots(9)$$

Determination of the Breaking Time of Evaporators' Helicoids Fan Blades

Determination of the Coefficient Kn

The dichotomy method was used to estimate the coefficient kn. Solving equation 3 was necessary in order to calculate the eigenvalues shown in Table 1. The results show that the eigenvalues increase with the increase of the index n.

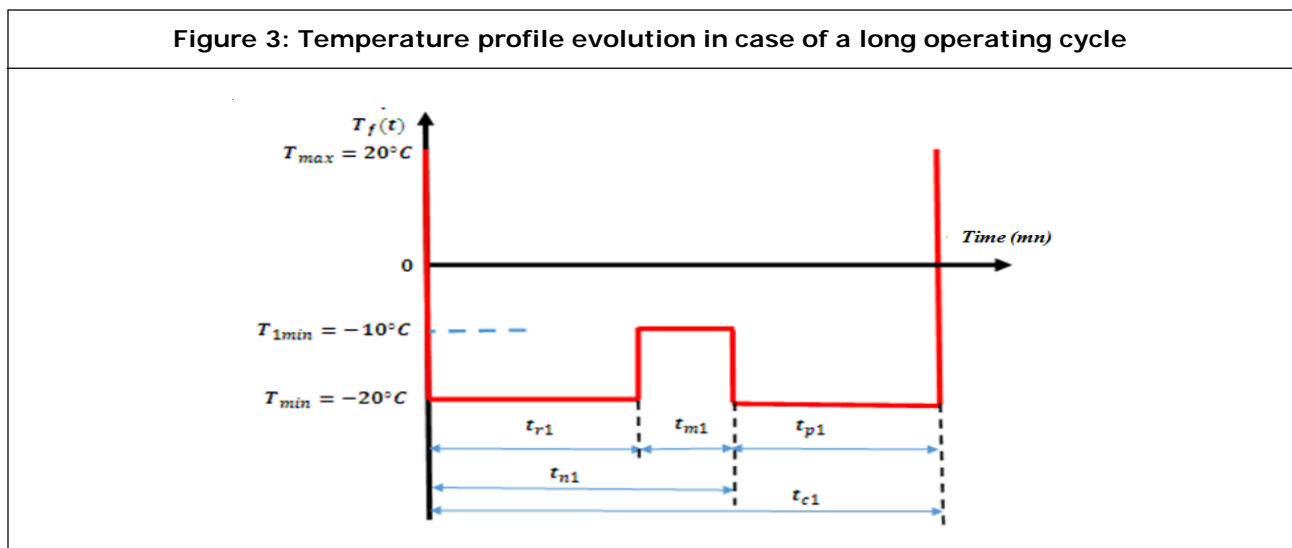


Table 1: Eigen Values of Equation

n	1	2	3	4	5	6	7	8
kn	1.5708	3.1417	6.2832	9.4248	12.5664	15.7080	21.9912	28.2743
n	9	10	11	12	13	14	15	16
kn	31.4159	59.6903	100.5310	131.9469	160.2212	163.3628	172.7876	175.9292

Temperature Profile Determination

Figures 4 and 5 show the evolution of the temperature field in the sample, respectively, when operating in the short cycle and the long cycle. We find that the temperature decreases in time and space from the edge to the heart of the sample. For the case of Figure 4, at $t = 0,004$ s the temperature at the heart ($x = 0$ mm) is over 28°C as it passes within -9°C at $t = 0.84$ s and at -20°C from the edge ($x = 0,005$ mm) at $t = 5,99$ s. When operating in the long cycle, at $t = 0.84$ s the sample's heart temperature is 28°C , it decreases more than 10°C at $t = 0,84$ s and less

than -5°C edge ($x = 0,005$ mm) at $t = 5,99$ s.

Determination of the Elastic Stress Profile Induced by the Thermal Gradient

Stress variations as a function of the position and time for the case of the short cycle and the case of the long cycle are shown respectively in Figures 6 and 7. The analysis of these figures shows that for relatively small amounts of time, the constraint is negative at the heart of the material and positive at the edge. This difference prevents expansions and compressions thus generating mechanical loads (Vincent *et al.*, 2005). Figure 6 shows the stress gradient

Figure 4: Evolution of the temperature field in the sample in case of short cycle

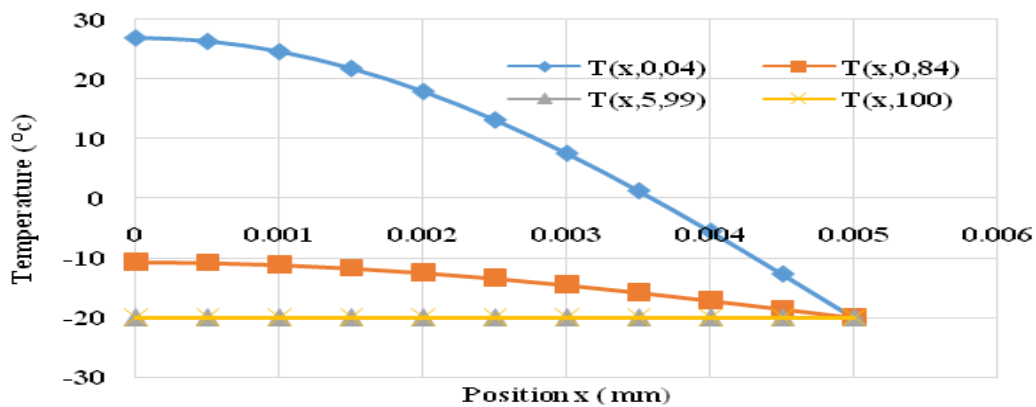


Figure 5: Evolution of the temperature field in the sample in case of long cycle

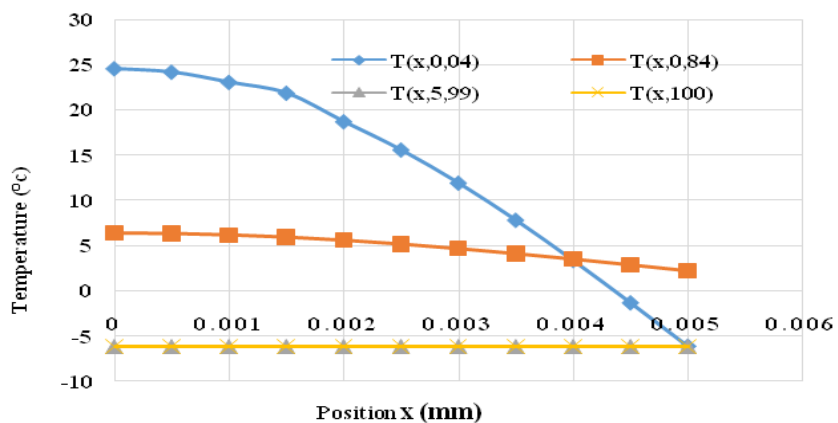


Figure 6: Stress variations as a function of the position and time for the case of the short cycle

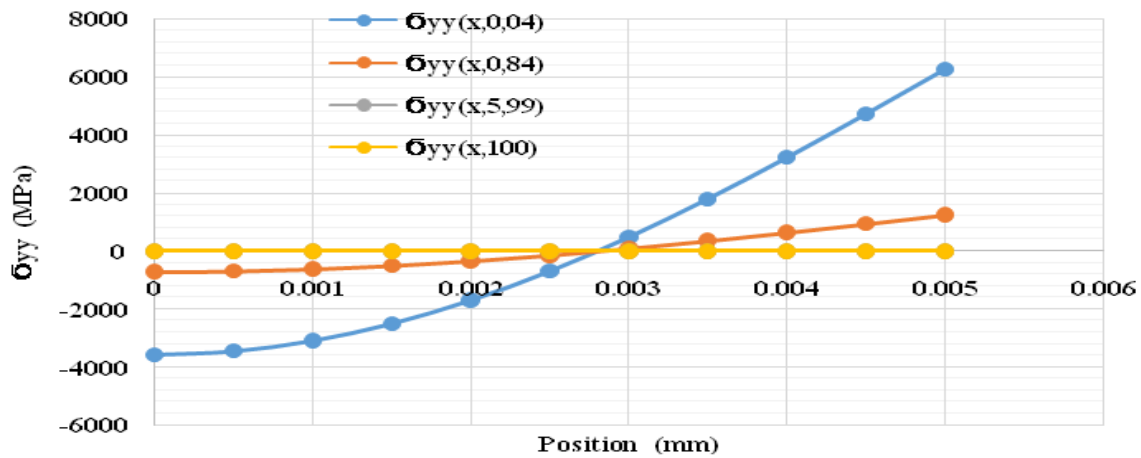
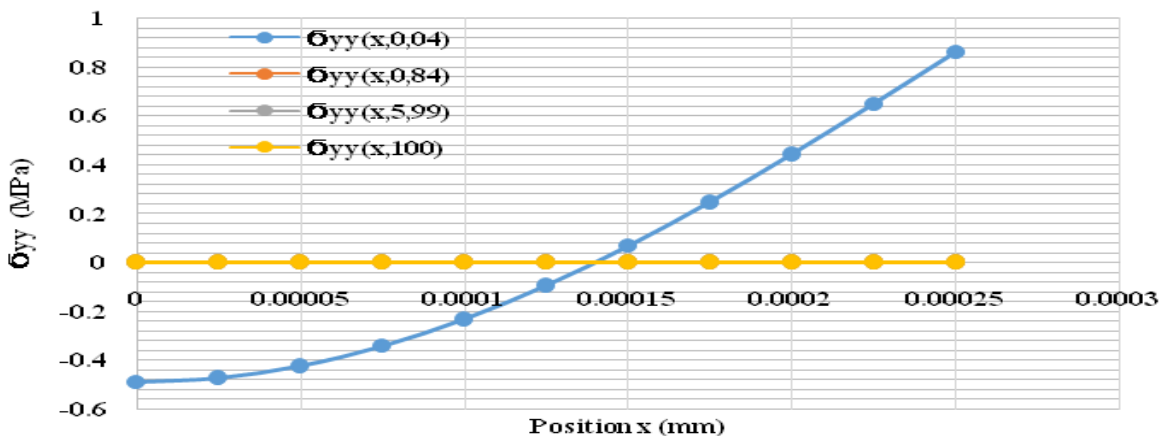


Figure 7: Stress variations as a function of the position and time for the case of the long cycle



between the edge and the heart are strongest at. It decreases at $t = 0.84s$, it is null when the temperature at heart and at the edge become homogeneous: it is said that the metal is cooled. In the case of Figure 7, we observe that the stress gradient between the edge and heart is maximal at . It becomes null from .

Determination of Stress Intensity Factor Profile

Figures 8 and 9 show the temperature variations induced by the elastic stress field of a surface

crack. The sample's surface is in tension when K is positive but for negative values of K , the sample's surface is in compression. This behavior of the material is called locking phenomenon during this part of the cycle (Hoai, 2009). Figure 8 curve shows that the temperature differential generates repeated cycles of warming and cooling at the surface of the evaporator fan, which explains the phenomenon of expansion and compression from which the mechanical loading originates. In the case of Figure 9, the analysis of

Figure 8: Temperature variation induced by the elastic stress field of a surface crack in case of short cycle

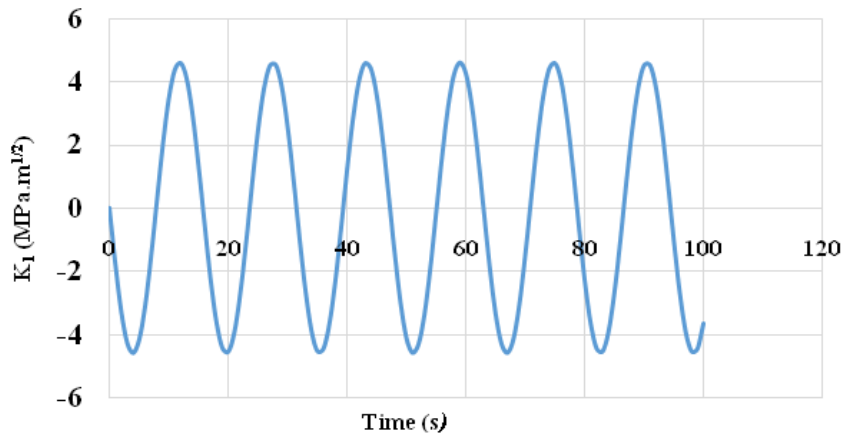
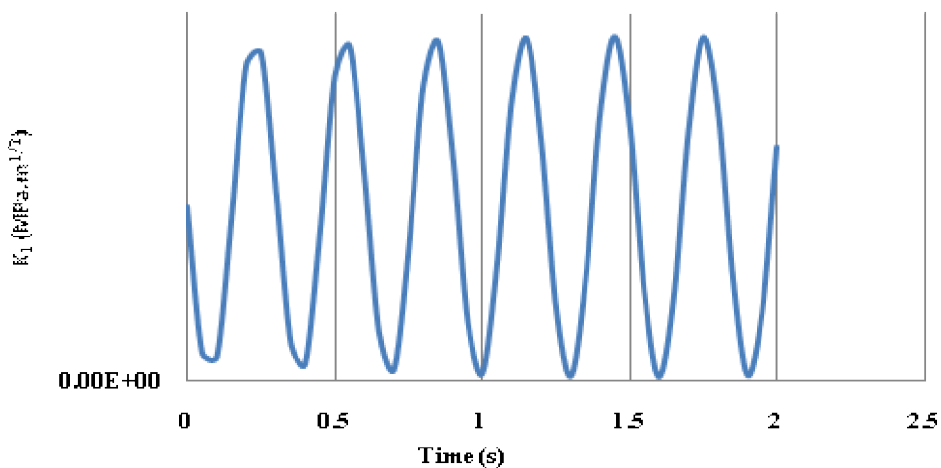


Figure 9: Temperature variation induced by the elastic stress field of a surface crack in case of long cycle



the curves shows there is no mechanical loading since the sample surface is tension (negligible cooling).

Determination of the Number of Complete Cycles and of the Blades Breaking Time

Knowing the maximum value of the stress intensity factor, we could determine the number of critical cycles before failure by solving the equation 6.

The breakup time will correspond to the period of a cycle increased by the number of critical cycles. It is given by Equation 7.

Short Cycle Case

The results indicate that the rupture of the blades will occur after a number of complete cycle $N_c = 3.10^{38}$ cycles.

The sudden break of evaporator fan blades will occur after.

Long Cycle Case

The results showed that the rupture of the blades will occur after a number of complete cycle $7,82.10^{40}$ cycles.

The sudden break of evaporator fan blades occur after.

In the end of this study, the cold room operating temperature fluctuations are not fully responsible for the breakdown of the metals that make up the fan blades.

CONCLUSION

Our objective was to study the influence of a negative cold room operating cycle on the evaporator fan blades. The results obtained show that the elastic stress created by the temperature field generates a mechanical loading on the surface of the fan blades. But this mechanical loading is negligible. The estimate of the blades breakup time indicates that, regardless of the operating cycle of the negative cold room (short cycle or long cycle), evaporator's axial fan blades will breakup even after hundreds of millions of year of operation. This leads us to conclude that the variation of thermal amplitude frequency have no mechanical effect on the metal blades of evaporator fan. Looking ahead, the combined effect of thermal shock and vibration will be the subject of future work.

REFERENCES

1. Hoai N L (2005), "*Etude de la propagation d'une fissure sous chargement thermique cyclique induisant un gradient de température dans l'épaisseur*", Thèse de Doctorat : école nationale supérieure de mécanique et d'aérotechnique, spécialité : Mécanique des Solides et des Matériaux. 273 pages.
2. Khama et al. (2009), "*Description mathématique du transfert de chaleur et de masse à travers un lit profond séchage. Effet du rétrécissement sur la porosité du lit*", Université des Frères Mentouri, Constantine, Algérie *Revue des Energies Renouvelables* Vol. 12 N°4 , pp. 597-605.
3. Lafarge M (2004), "*Modélisation couplée comportement endommagement et critères de rupture dans le domaine de la transition du PVDF*", Thèse de doctorat en Sciences et Génie des Matériaux, école Nationale Supérieure des Mines de Paris.
4. Laforte C (2001), "*Etude de l'adhérence de la glace sur des solides à caractères glaciophobes*", Mémoire de maîtrise, UQAC, p. 148.
5. Obrtlik K, Kruml T and Olakj P (1994), "Dislocation Structures in 316L Stainless Steel Cycled With Plastic Strain Amplitudes Over a Wide Interval", *Material Science and Engeneering*, A187, pp. 1-9.
6. Rice J R (1972), "Some remarks on elastic crack tip stress fields", *International Journal of Solids and Structures*, pp. 751-758.
7. Saanae M (2008), "*étude de la déformation plastique de la ferrite a basse température : simulations de dynamique des dislocations*", Thèse de doctorat en Physique et Chimie des Matériaux, université pierre et marie curie», Mémoire d'ingénieur de conception, école polytechnique centre de Thiès.
8. Tada H (1985), "The Stress Analysis of Cracks Handbook", Paris Productions Incorporated.
9. Tanguy B and Besson J (2012), "*Endommagement ductile des aciers:*

- identification des modèles à partir de l'expérimentation", Journée MECAMAT, rupture ductile, Centre des Matériaux, Mines Paris Tech, UMR CNRS763, p. 1CEA.*
10. Tavassoli A (1995), "Assessment of austenitic stainless steels", *Fusion Engineering and Design*, Vol. 29, pp. 371-390.
 11. Vincent (2006), "On the formation of crack networks in high cycle fatigue", *C R Mécanique*, Vol. 334, pp. 419-424.



International Journal of Engineering Research and Science & Technology

Hyderabad, INDIA. Ph: +91-09441351700, 09059645577

E-mail: editorijerst@gmail.com or editor@ijerst.com

Website: www.ijerst.com

